Biomedical Signal Processing and Control 31 (2017) 265–271

Contents lists available at ScienceDirect

Biomedical Signal Processing and Control

journal homepage: www.elsevier.com/locate/bspc

Measuring signal fluctuations in gait rhythm time series of patients with Parkinson's disease using entropy parameters

Yunfeng Wu[a,b,*], Pinnan Chen[a], Xin Luo[a], Meihong Wu[a], Lifang Liao[a], Shanshan Yang[a], Rangaraj M. Rangayyan[c]

[a] School of Information Science and Technology, Xiamen University, Xiamen, Fujian, China
[b] Fujian Key Laboratory of Sensing and Computing for Smart City Xiamen University, 422 Si Ming South Road, Xiamen, Fujian 361005, China
[c] Department of Electrical and Computer Engineering, Schulich School of Engineering, University of Calgary, Calgary, AB T2N 1N4, Canada

ARTICLE INFO

Article history:
Received 5 August 2015
Received in revised form 21 August 2016
Accepted 22 August 2016

Keywords:
Approximate entropy
Gait analysis
Generalized linear regression analysis
Parkinson's disease
Signal turns count
Stride time
Symbolic entropy

ABSTRACT

Gait rhythm disturbances due to abnormal strides indicate the degenerative mobility regulation of motor neurons affected by Parkinson's disease (PD). The aim of this work is to compute the approximate entropy (ApEn), normalized symbolic entropy (NSE), and signal turns count (STC) parameters for the measurements of stride fluctuations in PD. Generalized linear regression analysis (GLRA) and support vector machine (SVM) techniques were employed to implement nonlinear gait pattern classifications. The classification performance was evaluated in terms of overall accuracy, sensitivity, specificity, precision, Matthews correlation coefficient (MCC), and area under the receiver operating characteristic (ROC) curve. Our experimental results indicated that the ApEn, NSE, and STC parameters computed from the stride series of PD patients were all significantly larger (Wilcoxon rank-sum test: $p < 0.01$) than those of healthy control subjects. Based on the distinct features of ApEn, NSE, and STC, the SVM provided an accuracy rate of 84.48% and MCC of 0.7107, which are better than those of the GLRA (accuracy: 82.76%, MCC: 0.6552). The SVM and GLRA methods were able to distinguish PD gait patterns from healthy control cases with area of 0.9049 (SVM sensitivity: 0.7241, specificity: 0.9655) and 0.9037 (GLRA sensitivity: 0.8276, specificity: 0.8276) under the ROC curve, respectively, which are better or comparable with the classification results achieved by the other popular pattern classification methods.

1. Introduction

Parkinson's disease (PD) is a hypokinetic neurological disease due to apoptosis of dopaminergic cells in the substantia nigra [1]. The chronic deterioration of dopaminergic cells in the cerebrum decreases neural interactions such that neuronal signals are not properly transmitted from one neuron to another. The effects of PD may involve cognitive disorders, such as dementia, depression, disturbances in rapid eye movement sleep, visual difficulty, and dysphonia [2]. Degeneration of the central nervous system also leads to motor dysfunction, with the manifest symptoms in terms of noticeable tremor at 4–6 Hz, bradykinesia, postural instability, and rigidity [1]. Freezing of gait and impaired balance increase risks of falling for PD patients [3]. Lower limb stiffness, slow movement, small shuffling strides, and other apparent gait disturbances can be observed in PD patients with mild and moderate motor impairments [4].

Wearable sensors and portable mobility measurement systems are useful in ambulatory posture monitoring and gait assessment for PD patients [5–9]. Rigas et al. [10] and Salarian et al. [11] measured body movement activities by using a group of accelerometers to detect and quantify tremor and bradykinesia in PD. Patel et al. [6] set up a body sensor network with wearable sensors to fuse accelerometer data to estimate the severity of motor symptoms and other PD complications. Moore et al. [12] and Bachlin et al. [13] computed postural and kinematic features associated with freezing of gait from the acceleration signals recorded by inertial measurement systems. Su et al. [14] measured the asymmetry of frequency sub-band components of the ground reaction force time series to detect pathological gait patterns in Parkinson's disease. Corbier et al. [15] used autoregressive moving average models with reduced order using the Huberian approach to characterize the stochastic process of gait rhythm signals of patients with PD and Huntington's disease. Predominant gait features may provide meaningful information to assess the pathological condition [16–18] and evaluate

* Corresponding author at: School of Information Science and Technology, Xiamen University, Xiamen, Fujian, China.
E-mail address: y.wu@ieee.org (Y. Wu).

http://dx.doi.org/10.1016/j.bspc.2016.08.022
1746-8094/

the effects of anti-PD medicine intervention or physical therapy [19]. Hausdorff [20] emphasized the importance of fluctuations in stride process for movement disorder analysis.

In recent years, fractal analysis and statistical methods have been effectively applied to study the gait variability in neurological diseases [21–23]. Xia et al. [24] calculated the Lempel-Ziv complexity, fuzzy entropy, and Teager-Kaiser energy features to characterize the different gait patterns of patients with PD, amyotrophic lateral sclerosis, and Huntington's disease. Daliri [25] used the short-time Fourier transform to analyze the spectrum of gait signals, and computed the chi-square distances between the histograms of frequency variances for gait pattern classification. Ertugrul et al. [26] proposed the shifted 1D local binary patterns to characterize local disturbances in gait signals. Wahid et al. [27] quantified several spatial-temporal gait features for 23 PD patients and 26 age-matched healthy controls, and then compared the classification results of random forest, support vector machine (SVM), and kernel Fisher discriminant analysis methods. Lee and Lim [28] computed the wavelet transforms, and used a neural network with weighted fuzzy membership functions to distinguish pathological gait patterns in PD. Classification of gait patterns may assist neurologists to effectively identify and analyze the abnormal biomarkers related to movement disorders [29]. The motivation of this work is to compute the approximate entropy (ApEn), normalized symbolic entropy (NSE), and signal turns count (STC) features to measure the intrinsic irregularities as gait disturbance indicators in PD. The primary hypothesis is to test whether the gait rhythm irregularities in PD represented by these three features are significantly greater than those of age-matched healthy subjects. Based on the entropy and signal variability features, the Parkinsonian gait patterns can be effectively distinguished by different nonlinear classifiers.

2. Gait data set

The gait data used in the present study were provided by Yogev et al. [30], and can be accessed via the PhysioNet website [31]. 29 patients with idiopathic PD (20 males and nine females, age mean ± standard deviation (SD): 71.1 ± 8.1 years, body mass: 73.8 ± 15.7 kg, height: 169 ± 11 cm) and 29 age-matched healthy control (CO) subjects (16 males and 13 females, age: 71.9 ± 6.5 years, body mass: 73 ± 12.3 kg, height: 167 ± 8 cm) were recruited from the Tel-Aviv Sourasky Medical Center, Israel [30]. The neurological impairment stages of the PD patients ranged from 2 to 3 on the Hoehn and Yahr (H&Y) scale [32], which were confirmed by neurological examinations. The severity of PD was also quantified by the Unified Parkinson's Disease Rating Scale (UPDRS) [33]. The mean ± SD of the H&Y scale and UPDRS were 2.34 ± 0.4 and 32.9 ± 12.3 for the PD patients, respectively. The healthy control subjects were recruited from the local community in Tel-Aviv, Israel. All of the participants were able to ambulate independently, without a mobility-assistive device, and did not suffer from any other pathological condition, such as cardiovascular disease, respiratory disease, musculoskeletal disease, or other neurological disease. The subjects were requested to provide written informed consent. The experimental protocol and subject consent documents were approved by the Human Studies Committee of Tel-Aviv Sourasky Medical Center [30]. Data analysis methodology documents were reviewed and approved by the Ethics Committee of Xiamen University.

According to the experimental protocol of Yogev et al. [30], the subjects were asked to walk at their comfortable pace along a straight path on level ground for 2 min. The raw gait data were quantified by a force-sensitive system that contains a pair of shoes and a portable data acquisition module [34]. Each shoe contained eight ultrathin load sensors which measured vertical forces underneath the foot, with a sampling rate of 100 Hz and 12 bits per sample of quantizing resolution. The data acquisition module (dimensions: 19 × 14 × 4.5 cm; weight: 1.5 kg) was worn on the waist [34]. The gait cycle time series were processed using the algorithm proposed by Hausdorff et al. [35], which determines gait parameters such as stride time, stance time, and swing time. Although the stride time of both feet were recorded, we only considered the right-foot stride time for statistical analysis in the present study. To eliminate the start-up and ending effects of walking postures, which were somewhat different from the normal walking patterns, we excluded the first four strides (start-up from standing to initial walking) and the last four strides (from normal walking to ending the last stride) in the raw time series. A median filter [36,4] was applied to detect and remove the stride outliers, the amplitudes of which were 3 SD larger than the median value of the entire stride time series.

3. Gait rhythm analysis

3.1. Approximate entropy

The ApEn parameter, proposed by Pincus [37], is a statistical approach that measures the irregularity and subtle fluctuations in a physiological process [38]. For a stride-time series of N samples, $\{s(i)\}$, the ApEn model is expressed as ApEn(m, r, N), where the positive integer $m \in \mathbb{Z}^+$ denotes a window length for similarity comparison and the positive real number $r \in \Re^+$ is the tolerance parameter for accepting similarity matches [39]. Let us define a sequence of vectors, $\{\mathbf{x}^1(i), \mathbf{x}^2(i), \ldots, \mathbf{x}^{(N-m+1)}(i)\}$, in which each vector $\mathbf{x}^m(i) = [s(i), s(i+1), \ldots, s(i+m-1)]$ is composed of m consecutive data samples of the time series. The distance $d[\mathbf{x}^m(i), \mathbf{x}^m(j)]$ is defined as the maximum absolute difference between the corresponding elements from the vectors $\mathbf{x}^m(i)$ and $\mathbf{x}^m(j)$, respectively [40], i.e.,

$$d[\mathbf{x}^m(i), \mathbf{x}^m(j)] = \max_{k=1,2,\ldots,m} |s(i+k-1) - s(j+k-1)|. \quad (1)$$

For each i, $1 \leqslant i \leqslant N-m+1$, let $C_i^m(r)$ quantify the probability of j satisfying the condition that the distance between $\mathbf{x}^m(i)$ and the template $\mathbf{x}^m(j)$ is smaller than r, i.e.,

$$C_i^m(r) = \frac{\text{number of } j \text{ such that } d[\mathbf{x}^m(i), \mathbf{x}^m(j)] < r}{N-m+1}. \quad (2)$$

The value of $C_i^m(r)$ represents the frequency of similarity matches within a tolerance r between the vector $\mathbf{x}^m(i)$ of window length m and a given template $\mathbf{x}^m(j)$. Define the function $\phi^m(r)$ as the average of the natural logarithms of $C_i^m(r)$ [41]:

$$\phi^m(r) = \frac{\sum_{i=1}^{N-m+1} \ln C_i^m(r)}{N-m+1}. \quad (3)$$

Then, the approximate entropy ApEn(m, r) is given by [39]

$$\text{ApEn}(m, r) = \lim_{N\to\infty} [\phi^m(r) - \phi^{m+1}(r)]. \quad (4)$$

For a finite-length time series, the approximate entropy ApEn(m, r, N) is expressed as

$$\begin{aligned}\text{ApEn}(m, r, N) &= [\phi^m(r) - \phi^{m+1}(r)] \\ &= \frac{\sum_{i=1}^{N-m+1} \ln C_i^m(r)}{N-m+1} - \frac{\sum_{i=1}^{N-m} \ln C_i^{m+1}(r)}{N-m}. \end{aligned} \quad (5)$$

When N is much larger than m, that is $N \gg m$, the value of ApEn(m, r, N) can be approximately estimated as

$$\text{ApEn}(m, r, N) \approx \frac{\sum_{i=1}^{N-m} \ln \left[C_i^m(r)/C_i^{m+1}(r)\right]}{N-m}. \quad (6)$$

Typically, a small value of ApEn indicates that the time series possesses a high degree of regularity.

In the present study, we applied the ApEn(m, r, N) model to characterize the intrinsic irregularity of the stride rhythm of PD patients, as compared with healthy control subjects. The parameter $N = 65$ is the number of data samples in each stride time series (the first four and last four strides excluded), which is identical for all of the PD and CO subjects. The optimal combination of the ApEn model parameters $m = 2$ and $r = 0.03$ s was determined according to the two-sides Wilcoxon rank-sum test (or referred to as Mann–Whitney U test) results with the smallest p value. Instead of Student's t-test, the Wilcoxon rank-sum test was considered because it does not require the assumption of normal distributions [42], and its null hypothesis is that the statistical parameters of the CO subjects and PD patients are from the same group. The p value of the Wilcoxon rank-sum test indicates whether the gait parameters are different between the CO and PD subject groups over a level of statistical significance ($p < 0.01$).

3.2. Normalized symbolic entropy

Given a physiological process, symbolic dynamics probes the coarse graining of dynamics in the corresponding biomedical signal [43]. Fig. 1 shows the signal symbolization procedures, including quantization, segmentation of word sequences, histogram estimation, and entropy computation.

The parameters of symbolic dynamics are usually measured with the symbol sequence that can be converted from the time series with a certain threshold. With a predefined number of quantization levels q, the time series $\{s(i)\}$, $1 \le i \le N$, is converted into the symbol sequence $\{s^q(i)\}$, $1 \le i \le N$, the values of which are presented as integer labels from 0 to $q-1$. In the present study, we used the quantization level $q = 2$ to implement symbolized conversion of stride time series as

$$s^q(i) = \begin{cases} 1, & |s(i) - \bar{s}| \geqslant \theta, \\ 0, & |s(i) - \bar{s}| < \theta, \end{cases} \tag{7}$$

where $\bar{s}$ denotes the mean value of the stride-time series and θ is the quantization threshold. Next, we may define a word length L such that each word consists of L symbols as $s_L^q(i) = \{s^q(i), s^q(i-1), \cdots, s^q(i-L+1)\}$. When the quantization level q and the word length L are given, the total number of possible symbol combinations in a word is $M = q^L$ [43]. Therefore, we can calculate the probability of word occurrence in the symbol sequence $\{s_L^q(i)\}$ with

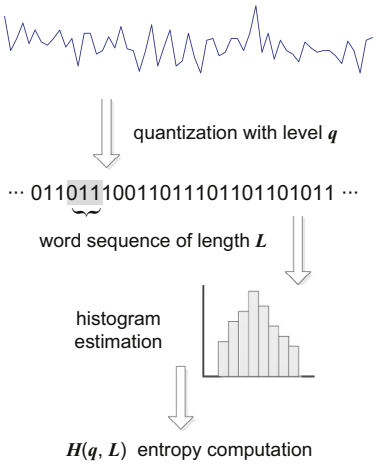

Fig. 1. Illustration of the signal symbolization procedure that involves quantization, word sequence segmentation, histogram estimation, and entropy computation.

a total of histogram bins $B = q^L$. The Shannon entropy is then computed as

$$H_s(q, L) = -\sum_{b=1}^{B} p_b(s_L^q) \log_2 \left[p_b(s_L^q) \right], \tag{8}$$

where $p_b(s_L^q)$ denotes the probability of word occurrence in each bin.

Eguia et al. [44] pointed out that the estimates of the empirical probabilities $p_b(s_L^q)$ are sometimes affected by random errors or a systematic bias. They reported that the correction of Shannon entropy should be modified with an additional systematic bias term as [44]

$$H_c(q, L) = H_s(q, L) + \frac{C_R - 1}{2M \ln 2}, \tag{9}$$

where C_R is the number of words that actually occur in the symbol sequence $\{s_L^q(i)\}$. The corrected Shannon entropy reaches its maximum value when all of the possible $M = q^L$ words occur with a uniform distribution in the symbol sequence [43] such that

$$H_c^{\max}(q, L) = \log_2 M + \frac{M - 1}{2M \ln 2}. \tag{10}$$

Then, NSE normalizes the corrected Shannon entropy as [43]:

$$H_n(q, L) = \frac{H_c(q, L)}{H_c^{\max}(q, L)} = \frac{H_s(q, L) + (C_R - 1)/(2M \ln 2)}{\log_2 M + (M - 1)/(2M \ln 2)}. \tag{11}$$

The symbolic entropy is normalized such that the entropy values computed from two symbol sequences with the same threshold and quantization levels but different word length L are also comparable [43]. To study the symbolic dynamics in the stride time series of healthy controls and PD patients, we set the word length parameter $L = 3$ such that the numbers of all possible words and histogram bins are $M = 8$ and $B = 8$, respectively. In our experiments, the optimal threshold parameter was set to be $\theta = 0.05$ s, which was selected according to the p value results (significance level: $p < 0.01$) of the two-sides Wilcoxon rank-sum hypothesis test.

3.3. Signal turns count

A signal turn is referred to as the time-series sample with waveform alteration in direction, i.e., the amplitude derivative changing from positive to negative or vice versa [45]. In order to eliminate the noise interference in temporal fluctuation analysis, we only consider the significant signal turns, the absolute value of amplitude difference between which and the preceding turn is over a threshold [4]. For a given signal, the identification of significant signal turns includes the following two steps:

1. **signal turn detection**: a signal turning sample $s(i)$ is detected and included in the turn sequence $\{t(n)\}$, if $[s(i) - s(i-1)][s(i+1) - s(i)] < 0, \quad 2 \le i \le N-1$;
2. **significant turn identification**: the significant turn $t(n)$ is identified if the difference between itself and the previous turn is greater than an assigned threshold τ, i.e., $\left| t(n) - t(n-1) \right| \ge \tau$; otherwise $t(n)$ should be excluded from the turn sequence.

The STC parameter accumulates the total number of significant signal turns identified. The STC parameter can be used to measure signal fluctuations with large amplitude changes in the time domain. In our experiments, the significant signal turns identification threshold τ was set to be 0.05 s, with the best gait pattern separation (two-sides Wilcoxon rank-sum hypothesis test $p < 0.01$) between healthy controls and PD patients.

4. Pattern analysis

4.1. Generalized linear regression analysis

Generalized linear regression analysis (GLRA) is an extension of the linear regression method. The GLRA combines a linear model part to represent systematic components and a probability distribution to represent random effects [46]. Because the stride patterns are expected to be categorized into only two subject groups, we applied the binomial distribution to estimate the binary outcomes (positive for PD group and negative for the control group, respectively). Therefore, the logit link function, the natural logarithm of an odds ratio, was used to express the relationship between the GLRA inputs and probability of occurrence of binary outcomes, μ, as

$$\ln\left(\frac{\mu}{1-\mu}\right) = \mathbf{f}^T\boldsymbol{\beta} = \beta_0 + \mathrm{f}_1\beta_1 + \cdots + \mathrm{f}_y\beta_y, \tag{12}$$

where $\boldsymbol{\beta}$ is the vector of regression coefficients (including the bias β_0), and $\mathbf{f}$ denotes the feature vector, $[1, \mathrm{f}_1, \cdots, \mathrm{f}_y]^T$, constructed with unity, ApEn, NSE, and STC parameters, for the GLRA inputs ($y = 3$). In our classification experiments, the maximum likelihood estimates of the GLRA coefficients were computed by the iterative weighted least squares procedure [47]. The optimal generalized linear regression coefficients obtained were $\boldsymbol{\beta}^* = [-7.14, -4.11, 1.38, 0.33]^T$, which is expected to help the GLRA achieve the largest area under the receiver operating characteristic (ROC) curve.

4.2. Support vector machine

Trained by supervised learning algorithms, the SVM is a type of nonlinear neural network model that implicitly transforms its inputs into a high-dimensional space with nonlinear kernels. The SVM methodology is established based on the Vapnik-Chervonenkis dimension theory [48], i.e., the network's learning is commonly achieved by minimizing structural risks. The SVM selects sufficient training data as support vectors to maximize the inter-class margin for pattern recognition. In order to produce a decision hyperplane in the high-dimensional mapped space, non-separable patterns are modified to be linearly separable with slack variables. The SVM model parameters were optimized by solving a constrained quadratic programming problem with equality constraints under the Karush-Kuhn-Tucker condition [49]. In our experiments, the input features for the SVM network were the same as those for the GLRA method, for the purpose of classification performance comparison. We used the Gaussian kernel function, $\varphi(\mathbf{f}, \mathbf{f}_k) = \exp\left(-\left\|\mathbf{f} - \mathbf{f}_k\right\|^2 / \sigma^2\right)$, to construct the nonlinear mapping in the high-dimensional space. The SVM training and testing steps were carried out with the MATLAB functions *svmtrain* and *svmclassification*. The Gaussian kernel function commonly makes the feature surface smoothing with an appropriate spread parameter. A small value of spread parameter would result in several local interpolations of feature surface, whereas a very large spread parameter would lower the interpolation accuracy in the feature space. The optimal spread parameter $\sigma = 3.6$ of the Gaussian kernel function was chosen in the range of [1, 50], with the highest value of area under the ROC curve provided by the SVM.

4.3. Classification performance evaluation

We used the leave-one-out cross-validation (LOO-CV) method to evaluate the generalization capability of the classifiers, such that every single subject's gait pattern can be separately categorized, without being involved in the training process.

The ROC curves were generated for the pattern classifiers, and the areas under the curve (AUC) were estimated to represent the diagnostic performance. The optimal cutoff point in the ROC curve for the binary classification decision of each classifier was determined according to the maximum value of Youden's index [50], J, i.e.,

$$\max J = \text{Sensitivity} + \text{Specificity} - 1. \tag{13}$$

The confusion matrix of each classifier was computed based on the optimal cutoff point of the ROC curve, to derive the true positive (TP), false positive (FP), true negative (TN), and false negative (FN) ratios. According to the confusion matrix, the parameters of sensitivity, specificity, precision (or positive predictive value), and overall accuracy were calculated.

In addition, Matthews correlation coefficient (MCC) [51] was computed as a quality indicator of gait pattern classification evaluation:

$$\text{MCC} = \frac{\text{TP} \times \text{TN} - \text{FP} \times \text{FN}}{\sqrt{P(1-P)S(1-S)}}, \tag{14}$$

$$P = \frac{(\text{TP} + \text{FP})}{(\text{TP} + \text{FP} + \text{TN} + \text{FN})}, \tag{15}$$

$$S = \frac{(\text{TP} + \text{FN})}{(\text{TP} + \text{FP} + \text{TN} + \text{FN})}. \tag{16}$$

The MCC measure takes into account all of the true and false positives and negatives, and is a type of correlation coefficient evaluation method for binary classification. MCC = 0 implies a classification equivalent to random guess. A positive value of MCC represents proper classification (+1 indicates perfect classification), whereas a negative MCC value implies poor classification worse than random guess (−1 indicates total disagreement between the predicted and actual groups) [51].

5. Results

Fig. 2 shows plots of the stride-time series recorded from a healthy CO subject (female, age: 78 years, height: 163 cm, gait speed: 1 m/s) and a patient with idiopathic PD (female, age: 68 years, height: 163 cm, gait speed: 1.05 m/s, H&Y scale: 2, UPDRS: 15), respectively. The significant signal turns with the absolute

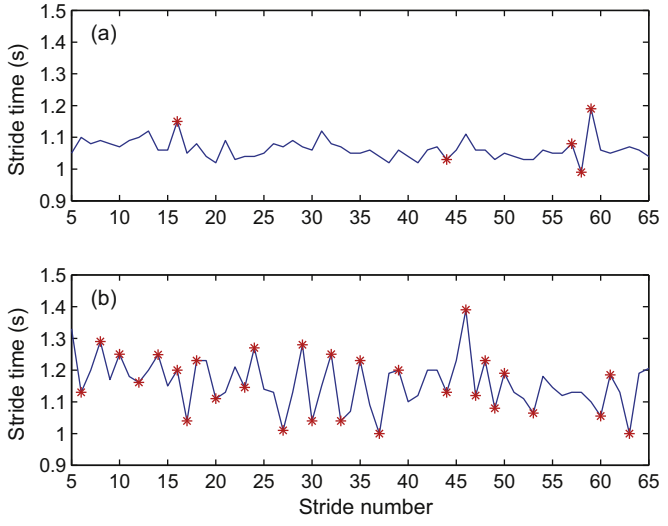

Fig. 2. Series of stride time recorded from (a) a 78-year-old healthy female subject and (b) a 68-year-old female patient with idiopathic PD (H&Y scale: 2, UPDRS: 15), respectively. Both stride-time series start from the 5th stride to avoid the start-up effects. Significant signal turns are marked by asterisks.

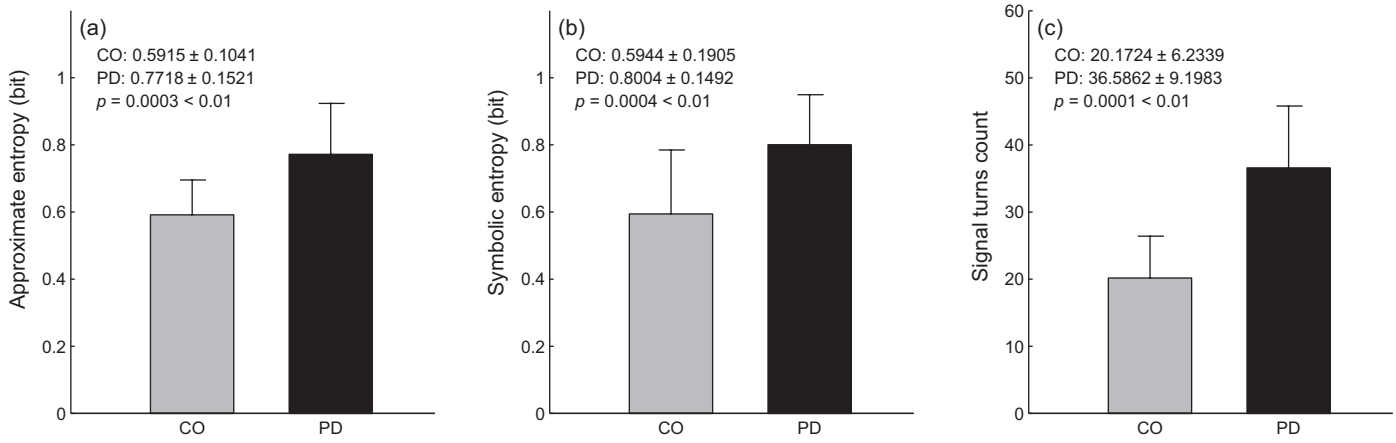

Fig. 3. Bar graphs of (a) approximate entropy (ApEn), (b) normalized symbolic entropy (NSE), and (c) signal turns count (STC) for healthy controls (CO) and patients with idiopathic Parkinson's disease (PD), respectively. Statistical significance level of the Wilcoxon rank-sum hypothesis test: $p < 0.01$.

amplitude changes over the threshold 0.05 s are marked by red asterisks. Although the gender, height, and gait speed of the PD patient and CO subject are matched, it is apparent in Fig. 2 that there are more significant signal turns identified in the stride series of the PD patient than those of the CO subject with comparable age.

The statistics of stride fluctuation parameters, i.e., ApEn, NSE, and STC, are provided in Fig. 3. The averaged ApEn value of PD patient group is 1.3 times larger than that of the CO subject group, which implies that PD patients commonly walk with much greater stride-to-stride irregularity. The NSE results show that the stride-time series of PD patients exhibit a higher degree of chaotic dynamics than that of healthy subjects.

The STC parameter that measures large signal amplitude changes is well-suited for characterizing the intrinsic fluctuations in stride series of PD patients. Larger gait rhythm fluctuations in PD lead to more significant signal turns in the series of stride time. It is clear from Fig. 3 that the average number of significant signal turns in PD subjects is much larger than that in healthy CO subjects, which characterizes the severe temporal oscillations in PD stride series, as illustrated in Fig. 2. Our results show that the stride-time STC values of PD patients with moderate balance impairment (H&Y scale: 3) are larger than those of PD patients with mild impairment (H&Y scale: 2 or 2.5). In addition, the mean values of ApEn, NSE, and STC are consistently larger with statistical significance ($p < 0.01$) for PD patients. The results indicate that the successive strides of PD patients generally contain abnormal variability or complexity patterns.

Details of the classification performance provided by the GLRA and SVM methods are tabulated in Table 1. The GLRA provided higher sensitivity (0.8276) than the SVM (0.7241), with three more (GLRA: 24 vs. SVM: 21) PD gait patterns being correctly recognized. However, the SVM correctly distinguished 28 gait patterns in the 29 CO subject group (specificity of 0.9655) and generated positive predictive value (or precision) of 0.9545, which are much better in comparison with the GLRA (specificity: 0.8276; precision: 0.8276). Regarding the overall classification results, the SVM was able to provide MCC of 0.7107 and AUC of 0.9049 (standard error, SE: 0.0382), which are consistently superior to those achieved by the GLRA method (MCC: 0.6552, AUC ± SE: 0.9037 ± 0.0396). The ROC curves produced by the two nonlinear classifiers shown in Fig. 4 confirm the superior classification performance of the SVM. We also computed the ROC results of the popular naive Bayes and k-nearest neighbor (k-NN, $k = 3$) classifiers, which were evaluated by the LOO-CV method as well. The area values under the ROC curve of naive Bayes and k-NN classifiers were 0.7931 and 0.8103, respectively, either of which is lower than that of the GLRA or SVM. In addition, we compared the classification results with several recent related studies [25–28] reported in the literature. Our SVM accuracy is better than the results of Lee an Lim [28] and Wahid et al. [27], and also comparable with Ertugrul et al. [26], as listed in Table 2. The present work contributes to the measure of ApEn, NSE, and STC, as new stride irregularity indicators associated with gait disturbance in PD. The entropy-based irregularity and temporal fluctuation features can assist the benchmark classifiers to achieve higher performance in automatic PD gait pattern recognition tasks.

Table 1
Classification results of the generalized linear regression analysis (GLRA) and support vector machine (SVM) methods for healthy and Parkinsonian stride process classification. Results are evaluated by the leave-one-out cross-validation method. AUC: area under the receiver operating characteristic curve; SE: standard error; MCC: Matthews correlation coefficient.

Classification results	GLRA	SVM
Accuracy	82.76%	84.48%
Sensitivity	0.8276	0.7241
Specificity	0.8276	0.9655
Precision	0.8276	0.9545
AUC ± SE	0.9037 ± 0.0396	0.9049 ± 0.0382
MCC	0.6552	0.7107

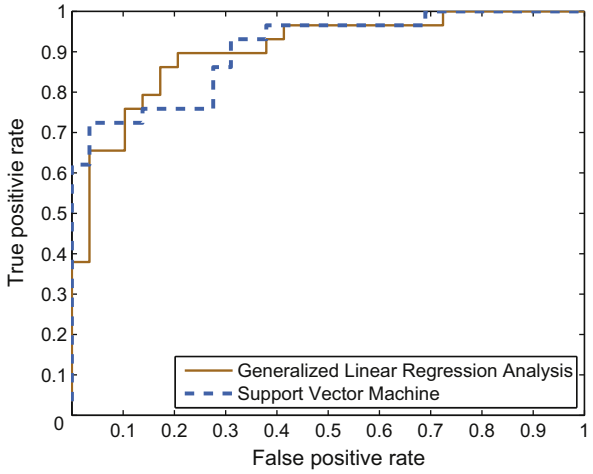

Fig. 4. Receiver operating characteristic (ROC) curves provided by the generalized linear regression analysis method (area under ROC curve: 0.9037) and the support vector machine (SVM) with Gaussian kernels (area under ROC curve: 0.9049).

Table 2
Comparisons of classification results with recent related studies on some open PD gait data sets. STC: signal turns count; SVM: support vector machine; AUC: area under the receiver operating characteristic curve; N/A: no applicable.

Reference	Gait parameters	Classifiers	Accuracy	Sensitivity	Specificity	AUC
Daliri [25]	Chi-square distance kernels	SVM	91.20%	0.9171	0.8992	N/A
Ertugrul et al. [26]	Shifted 1D local binary patterns	Multilayer perceptron	88.89%	0.889	0.822	N/A
Lee and Lim [28]	Wavelet transform coefficients	Fuzzy neural network	74.32%	0.8163	0.7377	N/A
Wahid et al. [27]	Spatial-temporal features	SVM	80.4%	0.8	0.82	0.85
Wahid et al. [27]	Spatial-temporal features	Random forest	92.6%	0.8	0.7	0.81
Our present study	ApEn, NSE, STC	SVM	84.48%	0.7241	0.9655	0.9049

6. Discussion and conclusion

In the present study, the nature of abnormal fluctuations in the stride series of PD patients was represented in terms of the ApEn, NSE, and STC parameters. The ApEn parameter compares the self-similarity matches of gait rhythm signals within a given tolerance level. The pathological gait rhythm series should exhibit a higher irregularity degree in terms of ApEn values. The ApEn parameter has the major advantage of adapting to a small number of signal samples (e.g., stride number $N < 100$ in the current series record), such that it is not necessary to require the subjects to perform long-term walking for gait monitoring. The ApEn parameter demands relatively lower computation cost, with favorable robustness to noise as well. A limitation of ApEn is that the entropy computing process avoids the occurrence of ln(0), which might result in some bias for a signal of a given length. Although sample entropy (SampEn) was commonly considered to demonstrate relative consistency to data length, Richman and Moorman [41] pointed out that the SampEn models would diverge from their predictions when the input data length is less than 100. On the other hand, the multiscale entropy proposed by Costa et al. [52] can be used with different types of entropy measures. Except for ApEn and SampEn, however, most of other entropy parameters, such as permutation entropy, are not suited for measuring the data with a small length, because the permutation entropy requires sufficient data samples to be permuted in sequence [53]. In the present work, the length of the stride series (i.e., the stride number) is equal for each subject, such that the ApEn bias effect for the subjects is small and comparable between one another. We did not use the empirical setting of ApEn parameter r equal to 0.1 times SD of each stride-time series, because such a parameter setting would result in subject-dependent ApEn models. Different gait rhythm time series may possess diverse ApEn values, because the SD of stride series varies from one subject to another. The identical ApEn parameter $r = 0.05$ s can be used as a physiological reference for both of PD and CO subject groups. In addition, it is worth noting that ApEn is fundamentally a statistical parameter to represent the "regularity" in a gait rhythm time series, not a direct quantitative index of physiological complexity. Our experimental results indicate that the stride-time series of PD patients show more irregular disturbances due to motor control disorders, which confirms the intuitional observations in Fig. 2.

The NSE measurement converts the signal samples into a set of word sequences, and then computes the Shannon entropy with respect to the probabilities of word sequences. It is explicit that the regular gait rhythm of healthy subjects should produce high frequency of particular word sequences, which may lead to relatively lower NSE values in comparison with those of PD patients. A proper setting of the quantization threshold value can help suppress the interference of random noise in the computation of the NSE parameter. As reported by Aziz and Arif [43], a small value of quantization threshold would measure noise-related variability, whereas a large value of NSE quantization threshold might not reveal the abnormal gait-rhythm dynamics in PD. In our experiments, the NSE parameter with the optimal quantization threshold of 0.05 s provided the best separation information between the health control and PD subject groups.

The present work has some limitations as well. Although the PhysioNet gait database contains some PD stride series in response to different types of dual tasking, we included in the experiments only the stride series performed by subjects at their comfortable walking pace, because we only focus on the effects of PD motor impairment on gait disturbances during typical walking. In this study, we only focus on the right-foot stride dynamics of each subject, because the left-foot and right-foot stride dynamics of the CO subjects are quite similar, and most of the PD patients are without impairment of balance (H&Y scale <3). Nevertheless, the ApEn, NSE, and STC results consistently indicate a significantly higher degree of stride fluctuations in PD patients than in CO subjects. The GLRA and SVM classifiers can successfully distinguish most of the gait patterns of PD patients from those of healthy controls, which also demonstrates the effectiveness of our gait analysis methods.

As emphasized by Montero-Odasso et al. [54] and Hausdorff [55], gait analysis is a potential complementary approach for understanding the interrelationships between movement disorders and neurological dysfunction. In this work, we computed the ApEn, NSE, and STC parameters as important indicators of gait disturbances in PD. The SVM and GLRA methods are useful for effective automatic PD gait pattern classifications, which may improve the assessment of PD progression in clinical practice. In the future work, advanced temporal and fractal analysis methods [56,57] could also be considered for fluctuation representations of gait patterns associated with movement disorders.

Competing interests

There is no conflict of interest.

Ethical approval

The experimental protocol and subject consent documents were approved by the Human Studies Committee of Tel-Aviv Sourasky Medical Center. Data analysis methodology documents were reviewed and approved by the Ethics Committee of Xiamen University.

Acknowledgments

The authors would like to thank the anonymous reviewers for their valuable comments and Ms. Hang Zhang for technical assistance. The authors also appreciate Galit Yogev, Nir Giladi, Chava Peretz, Shmuel Springer, Ely S. Simon, and Jeffrey M. Hausdorff, for providing the gait data. This work was supported by the National Natural Science Foundation of China (grant numbers: 31200769 and 81101115). Yunfeng Wu and Meihong Wu were supported by the Program for New Century Excellent Talents in Fujian Province University. Rangaraj M. Rangayyan was supported by the High-Level Foreign Experts Program of the State Administration of Foreign Experts Affairs in China.

References

[1] J. Jankovic, Parkinson's disease: clinical features and diagnosis, J. Neurol. Neurosurg. Psychiatry 79 (2008) 368–376.
[2] S. Yang, F. Zheng, X. Luo, S. Cai, Y. Wu, K. Liu, M. Wu, J. Chen, S. Krishnan, Effective dysphonia detection using feature dimension reduction and kernel density estimation for patients with Parkinson's disease, PLOS ONE 9 (2014) e88825.
[3] B.R. Bloem, J.M. Hausdorff, J.E. Visser, N. Giladi, Falls and freezing of gait in Parkinson's disease: a review of two interconnected, episodic phenomena, Mov. Disord. 19 (2004) 871–884.
[4] Y. Wu, S. Krishnan, Statistical analysis of gait rhythm in patients with Parkinson's disease, IEEE Trans. Neural Syst. Rehabil. Eng. 18 (2010) 150–158.
[5] S.R. Hundza, W.R. Hook, C.R. Harris, S.V. Mahajan, P.A. Leslie, C.A. Spani, L.G. Spalteholz, B.J. Birch, D.T. Commandeur, N.J. Livingston, Accurate and reliable gait cycle detection in Parkinson's disease, IEEE Trans. Neural Syst. Rehabil. Eng. 22 (2014) 127–137.
[6] S. Patel, K. Lorincz, R. Hughes, N. Huggins, J. Growdon, D. Standaert, M. Akay, J. Dy, M. Welsh, P. Bonato, Monitoring motor fluctuations in patients with Parkinson's disease using wearable sensors, IEEE Trans. Inf. Technol. Biomed. 13 (2009) 864–873.
[7] I. Tien, S.D. Glaser, R. Bajcsy, D.S. Goodin, M.J. Aminoff, Results of using a wireless inertial measuring system to quantify gait motions in control subjects, IEEE Trans. Inf. Technol. Biomed. 14 (2010) 904–915.
[8] L. Palmerini, L. Rocchi, S. Mellone, F. Valzania, L. Chiari, Feature selection for accelerometer-based posture analysis in Parkinson's disease, IEEE Trans. Inf. Technol. Biomed. 15 (2011) 481–490.
[9] M. Yoneyama, Y. Kurihara, K. Watanabe, H. Mitoma, Accelerometry-based gait analysis and its application to Parkinson's disease assessment-Part 2: a new measure for quantifying walking behavior, IEEE Trans. Neural Syst. Rehabil. Eng. 21 (2013) 999–1005.
[10] G. Rigas, A.T. Tzallas, M.G. Tsipouras, P. Bougia, E.E. Tripoliti, D. Baga, D.I. Fotiadis, S.G. Tsouli, S. Konitsiotis, Assessment of tremor activity in the Parkinson's disease using a set of wearable sensors, IEEE Trans. Inf. Technol. Biomed. 16 (2012) 478–487.
[11] A. Salarian, H. Russmann, C. Wider, P.R. Burkhard, F.J.G. Vingerhoets, K. Aminian, Quantification of tremor and bradykinesia in Parkinson's disease using a novel ambulatory monitoring system, IEEE Trans. Biomed. Eng. 54 (2007) 313–322.
[12] S.T. Moore, H.G. MacDougall, W.G. Ondo, Ambulatory monitoring of freezing of gait in Parkinson's disease, J. Neurosci. Methods 167 (2008) 340–348.
[13] M. Bachlin, M. Plotnik, D. Roggen, I. Maidan, J.M. Hausdorff, N. Giladi, G. Troster, Wearable assistant for Parkinson's disease patients with the freezing of gait symptom, IEEE Trans. Inf. Technol. Biomed. 14 (2010) 436–446.
[14] B.L. Su, R. Song, L.Y. Guo, C.W. Yen, Characterizing gait asymmetry via frequency sub-band components of the ground reaction force, Biomed. Signal Process. Control 18 (2015) 56–60.
[15] C. Corbier, M. El Badaoui, H.M.R. Ugalde, Huberian approach for reduced order ARMA modeling of neurodegenerative disorder signal, Signal Process. 113 (2015) 273–284.
[16] M. Plotnik, Y. Dagan, T. Gurevich, N. Giladi, J.M. Hausdorff, Effects of cognitive function on gait and dual tasking abilities in patients with Parkinson's disease suffering from motor response fluctuations, Exp. Brain Res. 208 (2011) 169–179.
[17] S. Lord, K. Baker, A. Nieuwboer, D. Burn, L. Rochester, Gait variability in Parkinson's disease: an indicator of non-dopaminergic contributors to gait dysfunction? J. Neurol. 258 (2011) 566–572.
[18] Y. Wu, X. Luo, P. Chen, L. Liao, S. Yang, R.M. Rangayyan, Forward autoregressive modeling for stride process analysis in patients with idiopathic Parkinson's disease, in: Proceedings of the 10th IEEE International Symposium on Medical Measurement and Applications, Torino, Italy, 2015, pp. 349–352.
[19] J.M. Hausdorff, J. Lowenthal, T. Herman, L. Gruendlinger, C. Peretz, N. Giladi, Rhythmic auditory stimulation modulates gait variability in Parkinson's disease, Eur. J. Neurosci. 26 (2007) 2369–2375.
[20] J.M. Hausdorff, Gait dynamics, fractals and falls: finding meaning in the stride-to-stride fluctuations of human walking, Hum. Mov. Sci. 26 (2007) 555–589.
[21] A. Salarian, H. Russmann, F.J.G. Vingerhoets, C. Dehollain, Y. Blanc, P.R. Burkhard, K. Aminian, Gait assessment in Parkinson's disease: toward an ambulatory system for long-term monitoring, IEEE Trans. Biomed. Eng. 51 (2004) 1434–1443.
[22] J.M. Hausdorff, Gait dynamics in Parkinson's disease: common and distinct behavior among stride length, gait variability, and fractal-like scaling, Chaos 19 (2009) 026113.
[23] D.C. Dewey, S. Miocinovic, I. Bernstein, P. Khemani, R.B. Dewey III, R. Ross Querry, S. Chitnis, R.B. Dewey Jr., Automated gait and balance parameters diagnose and correlate with severity in Parkinson disease, J. Neurol. Sci. 345 (2014) 131–138.
[24] Y. Xia, Q. Gao, Q. Ye, Classification of gait rhythm signals between patients with neuro-degenerative diseases and normal subjects: experiments with statistical features and different classification models, Biomed. Signal Process. Control 18 (2015) 254–262.
[25] M.R. Daliri, Chi-square distance kernel of the gaits for the diagnosis of Parkinson's disease, Biomed. Signal Process. Control 8 (2013) 66–70.
[26] O.F. Ertugrul, Y. Kaya, R. Tekin, M.N. Almali, Detection of Parkinson's disease by shifted one dimensional local binary patterns from gait, Expert Syst. Appl. 56 (2016) 156–163.
[27] F. Wahid, R.K. Begg, C.J. Hass, S. Halgamuge, D.C. Ackland, Classification of Parkinson's disease gait using spatial-temporal gait features, IEEE J. Biomed. Health Inform. 19 (2015) 1794–1802.
[28] S.H. Lee, J.S. Lim, Parkinson's disease classification using gait characteristics and wavelet-based feature extraction, Expert Syst. Appl. 39 (2012) 7338–7344.
[29] Y. Wu, L. Shi, Analysis of altered gait rhythm in amyotrophic lateral sclerosis based on nonparametric probability density function estimation, Med. Eng. Phys. 33 (2011) 347–355.
[30] G. Yogev, N. Giladi, C. Peretz, S. Springer, E.S. Simon, J.M. Hausdorff, Dual tasking, gait rhythmicity, and Parkinson's disease: which aspects of gait are attention demanding? Eur. J. Neurosci. 22 (2005) 1248–1256.
[31] G.B. Moody, R.G. Mark, A.L. Goldberger, PhysioNet: a web-based resource for the study of physiologic signals, IEEE Eng. Med. Biol. Mag. 20 (2001) 70–75.
[32] M.M. Hoehn, M.D. Yahr, Parkinsonism: onset, progression, and mortality, Neurology 17 (1967) 427–442.
[33] C.G. Goetz, W. Poewe, O. Rascol, C. Sampaio, G.T. Stebbins, S. Fahn, A.E. Lang, P. Martinez-Martin, B. Tilley, B. Van Hilten, C. Kleczka, L. Seidl, The unified Parkinson's disease rating scale (UPDRS): status and recommendations, Mov. Disord. 18 (2003) 738–750.
[34] S. Frenkel-Toledo, N. Giladi, C. Peretz, T. Herman, L. Gruendlinger, J.M. Hausdorff, Treadmill walking as an external pacemaker to improve gait rhythm and stability in Parkinson's disease, Mov. Disord. 20 (2005) 1109–1114.
[35] J.M. Hausdorff, Z. Ladin, J.Y. Wei, Footswitch system for measurement of the temporal parameters of gait, J. Biomech. 28 (1995) 347–351.
[36] Y. Wu, S. Krishnan, Computer-aided analysis of gait rhythm fluctuations in amyotrophic lateral sclerosis, Med. Biol. Eng. Comput. 47 (2009) 1165–1171.
[37] S.M. Pincus, Approximate entropy as a measure of system complexity, Proc. Natl. Acad. Sci. U. S. A. 88 (1991) 2297–2301.
[38] W. Chen, J. Zhuang, W. Yu, Z. Wang, Measuring complexity using FuzzyEn, ApEn, and SampEn, Med. Eng. Phys. 31 (2009) 61–68.
[39] S.M. Pincus, A.L. Goldberger, Physiological time-series analysis: what does regularity quantify? Am. J. Physiol. 266 (1994) 1643–1656.
[40] S.M. Pincus, Approximate entropy (ApEn) as a complexity measure, Chaos 5 (1995) 110–117.
[41] J.S. Richman, J.R. Moorman, Physiological time-series analysis using approximate entropy and sample entropy, Am. J. Physiol. 278 (2000) 2039–2049.
[42] Y. Wu, P. Chen, X. Luo, H. Huang, L. Liao, Y. Yao, M. Wu, R.M. Rangayyan, Quantification of knee vibroarthrographic signal irregularity associated with patellofemoral joint cartilage pathology based on entropy and envelope amplitude measures, Comput. Methods Prog. Biomed. 130 (2016) 1–12.
[43] W. Aziz, M. Arif, Complexity analysis of stride interval time series by threshold dependent symbolic entropy, Eur. J. Appl. Physiol. 98 (2006) 30–40.
[44] M.C. Eguia, M.I. Rabinovich, H.D.I. Abarbanel, Information transmission and recovery in neural communication channels, Phys. Rev. E 62 (2000) 7111–7122.
[45] R.M. Rangayyan, Y. Wu, Analysis of vibroarthrographic signals with features related to signal variability and radial-basis functions, Ann. Biomed. Eng. 37 (2009) 156–163.
[46] A.J. Dobson, A. Barnett, An Introduction to Generalized Linear Models, 3rd ed., CRC Press, Boca Raton, FL, 2008.
[47] A. Charnes, E.L. Frome, P.L. Yu, The equivalence of generalized least squares and maximum likelihood estimates in the exponential family, J. Am. Stat. Assoc. 71 (1976) 169–171.
[48] C.J.C. Bugers, A tutorial on support vector machines for pattern recognition, Data Min. Knowl. Discov. 2 (1998) 121–167.
[49] V.N. Vapnik, Statistical Learning Theory, Wiley, New York, NY, 1998.
[50] W.J. Youden, Index for rating diagnostic tests, Cancer 3 (1950) 32–35.
[51] P. Baldi, S. Brunak, Y. Chauvin, C.A.F. Andersen, H. Nielsen, Assessing the accuracy of prediction algorithms for classification: an overview, Bioinformatics 16 (2000) 412–424.
[52] M. Costa, A.L. Goldberger, C.-K. Peng, Multiscale entropy analysis of complex physiologic time series, Phys. Rev. Lett. 89 (2002) 062102.
[53] C. Bandt, B. Pompe, Permutation entropy: a natural complexity measure for time series, Phys. Rev. Lett. 88 (2002) 174102.
[54] M. Montero-Odasso, J. Verghese, O. Beauchet, J.M. Hausdorff, Gait and cognition: a complementary approach to understanding brain function and the risk of falling, J. Am. Geriatr. Soc. 60 (2012) 2127–2136.
[55] J.M. Hausdorff, N.B. Alexander, Gait Disorders: Evaluation and Management, Informa Healthcare, New York, NY, 2005.
[56] S. Yang, S. Cai, F. Zheng, Y. Wu, K. Liu, M. Wu, Q. Zou, J. Chen, Representation of fluctuation features in pathological knee joint vibroarthrographic signals using kernel density modeling method, Med. Eng. Phys. 36 (2014) 1305–1311.
[57] M. Wu, L. Liao, X. Luo, X. Ye, Y. Yao, P. Chen, L. Shi, H. Huang, Y. Wu, Analysis and classification of stride patterns associated with children development using gait signal dynamics parameters and ensemble learning algorithms, BioMed. Res. Int. 2016 (2016) 9246280.